

Equipartition and ergodicity in closed one-dimensional systems of hard spheres with different masses

Graeme J. Ackland

Department of Physics, University of Edinburgh, EH9 3JZ, Scotland

(Received 23 March 1992; revised manuscript received 25 September 1992)

We show by computer simulation that a one-dimensional closed system of hard spheres with different masses exhibits equipartition. This is true even when the system contains as few as two particles or is nonergodic. Use of periodic boundary conditions gives very different results from the fixed boundaries. For more than two particles, it is shown that, for most mass ratios, the probability of an exact return to the initial state is vanishingly small. The density of states in momentum space accessible by a particular particle corresponds to a uniform density of states in the region allowed by conservation laws. There are special mass ratios for which ergodicity fails and recurrence occurs. Even for these nonergodic cases, equipartition is obtained. The free volume available to each particle is independent of its mass. These results are in contrast with numerous studies of systems using soft, anharmonic interactions and have implications regarding equipartition in molecular-dynamic simulations.

PACS number(s): 05.20.Dd, 05.60.+w

I. INTRODUCTION

It is a common assumption that periodic boundary conditions are a realistic means with which to carry out atomistic simulations, provided that individual particles do not interact with their own images. Thus interactions are assumed to drop off faster than $1/r^2$, such that a large enough system will enable finite-size effects to be discounted. Moreover, systems are often assumed to exhibit ergodicity and equipartition. Herein we investigate the validity of these two assumptions by computer simulations and matrix analysis of a simple system.

A vast amount of analytic and simulation work has been done on nonlinear lattices [1,2] starting with the Fermi-Pasta-Ulam (FPU) recurrence problem [3]. Most related work has concentrated on systems with identical particles [4,5]. There seems to be a general trend toward ergodicity with increasing numbers of particles and increased energy [6,7]. Ergodicity has been shown to be violated in a small system of two particles with fixed boundaries, for some low energy configurations, because periodic solutions exist [8]. With the increased complexity of a third particle these authors were unable to find a nonergodic regime.

Here, we examine a different case, which has implications for finite-sized molecular-dynamic (MD) simulations; that of equipartition and ergodicity in a small one-dimensional system of hard spheres with different masses. Comparison with previous work using nonlinear interactions, such as the Lennard-Jones potential [9,10] can be made by assuming the hard-sphere regime as being the high-energy limit, at which the interaction is most anharmonic and the attractive part of the potential is negligible.

This study is complimentary to a previous study [11] which examined systems of hundreds of particles with two masses to determine the kinetics of going from a highly nonequilibrium state to a Boltzmann distribution.

Since we are working in one dimension the ordering of the particles around the ring is conserved. We shall also work throughout in the center of mass reference frame. These two conditions make it impossible for all the particles to sample all of position space, so we will define the phase space only in terms of the momentum variables and use ergodicity to refer to sampling of the momentum space only. Note that this is not the standard definition applied in higher dimensions where ordering is not conserved.

The hard-sphere potential enables the evolution to be described by a series of discrete collisions and mapped onto a group of matrices. The hard-sphere system allows enormous computational simplicity. This is essential because ergodicity can be reliably tested with about 10^6 sampled microstates. The time taken to reach equipartition scales rapidly with the frequency of the normal modes [12], so the present case would be expected to equilibrate rapidly. With a large range of possible mass ratios and numbers of particles it is important to examine many different cases. Moreover, because we are using hard spheres (no energy scale) the system is athermal, so there is no need to examine the possibility of different temperature regimes.

A physical realization of the system might be a set of frictionless balls moving around a closed loop.

The system can, without loss of generality, be viewed in the center of mass frame. As in previous work [11] the particle radii were set to zero. This has no effect on the energetics but has a trivial effect on the range of motion [13], as discussed in Sec. V. There are thus two constraints applied to the system—conservation of momentum and of energy. Writing the momentum and mass of particle i as p_i and m_i , respectively, we have

$$\sum_i p_i = 0, \quad \sum_i p_i^2 / 2m_i = E. \quad (1)$$

Closed systems of this kind are frequently used to mod-

el much larger systems, the system being viewed as periodically repeating (periodic boundary conditions).

Herein, we examine the time-averaged energy per atom to study the onset of equipartition. Ergodicity in momentum space is tested by plotting histograms of momentum against the time for which a particle has that momentum. The free volume is measured by finding the mean position of each particle, its rms deviation from that position, and its probability distribution. These averages are convergent because the overall angular momentum is zero. Finally, we examine a number of special nonergodic cases and present a matrix method to explain their nonergodicity in terms of a chaotic walk.

II. EQUIPARTITION WITH PERIODIC BOUNDARY CONDITIONS

The calculation considers a number of hard spheres on a one-dimensional 1D closed ring. At each step, the time to the next collision between each pair of particles is calculated, the smallest such time is used as a time step to move all the particles, and the velocities of the two colliding particles are updated so as to conserve energy and momentum. In one dimension, for a collision between two particles, masses m_A and m_B with initial velocities u_A and u_B , the new velocity of m_A is

$$v_A = \frac{(m_A - m_B)u_A + 2m_B u_B}{m_A + m_B}. \quad (2)$$

After a single collision, the next time step is calculated and the process is repeated.

We have carried out a series of computer calculations with randomly chosen initial velocities, and initial positions. Initially, the masses of the various particles were chosen to be small integers to make it easier to spot relationships between various properties. For the same reason, these are the runs which are depicted in the various figures. These lead to the result that at equilibrium, when viewed in the center of mass reference frame, the mean energy of a particle, averaged over time, is proportional to the mass of all other particles in the system. Subsequently we also ran tests in which masses in the range 0–1 were generated randomly by the computer, and these runs gave the same results, showing the choice of integer masses is usually unimportant (though see Sec. VI).

We note that equilibrium tends to take longer to reach if the particles are of very different masses because of the small transfer of energy in elastic collisions. We have considered both small-integer mass ratios and “irrational” (to computational precision) ratios and find that this makes no difference.

For two particles the collision rules allow only two states. In this case Eq. (3) can be obtained analytically. Also notice that the standard equipartition result $\langle E_i \rangle = E/N$ is obtained in three cases:

- (1) The number of particles becomes very large: $\sum_j m_j \gg m_i$.
- (2) One of the particle masses becomes infinite (equivalent to a fixed boundary).
- (3) All particles have the same mass:

$$[\sum_j m_j - m_i] / [\sum_j m_j] = (N-1)/N \text{ (a constant).}$$

The rule relating mean energy to masses has been found to hold good for all systems containing two or more particles, including those which are not ergodic,

$$\langle E_i \rangle = \frac{\sum_j m_j - m_i}{\sum_j m_j} \frac{E}{N-1}. \quad (3)$$

This is the result obtained by statistical mechanics in the “molecular-dynamics” ensemble in which energy, momentum, volume, and the number of particles are conserved [14]. This ensemble leads to projected densities of states equivalent to those found here. Derivation of Eq. (3) therefrom is discussed in Sec. III.

We note, however, that the ensemble averaging in this method presupposes an ergodic system. As we shall see, Eq. (3) holds not only in the ergodic cases, but also in the “special” nonergodic cases discussed in Sec. VI.

Equation (3) can be viewed as a modification of the equipartition law for a finite system, arising as consequence of conservation of momentum, since periodic boundary conditions rigorously enforce conservation of momentum. Fixed boundaries, of course, do not.

Thus we have shown that a consequence of the effect of periodic boundaries is to reduce the apparent energy in low momentum modes. This is a feature which has always been overlooked in molecular-dynamics simulations.

Consequences for molecular dynamics

This result is of general validity and will affect the occupation of various phonon modes in molecular-dynamics calculations. Note that for very large systems, or for systems of identical particles (but see below for the case of molecules with rotational degrees of freedom), the standard equipartition result is obtained, hence the above can be regarded as a finite-size effect. Moreover, for a system with rigid boundaries we can regard the boundary as an infinitely massive extra particle, in which case Eq. (3) again leads to equipartition of energy among the other particles within the center of mass frame. A similar argument applies to rotational degrees of freedom in a molecular-dynamics simulation:

$$\langle i_i \omega^2 / 2 \rangle = (I - i_i) kT / I, \quad (4)$$

where i_i is the moment of inertia of the i th molecule and I is the moment of inertia of the whole system. I is typically about axes through the simulation cell center, because these are the axes about which rotation is suppressed in molecular-dynamics simulations. We can see that

$$\langle m u_i^2 \rangle / \langle i_i \omega^2 \rangle = (1 - m_i / M) / (1 - i_i / I). \quad (5)$$

Since M is simply a sum of constituent masses, while I incorporates the distance from the cell axis (in general this is bigger than the distance from the molecular axis),

$$m_i / M > i_i / I, \quad (6)$$

whence

$$\langle mu_i^2 \rangle / \langle i_i \omega^2 \rangle < 1. \quad (7)$$

Hence for a finite-size MD system we would expect the periodic boundary conditions to lead to a larger energy (temperature) associated with the rotational degrees of freedom than that associated with the translational. This has in fact been observed [15] but not previously explained. Once again, as the number of particles tends to infinity the effect vanishes.

III. DENSITY OF STATES—ERGODICITY

In one dimension the ordering of particles around a ring cannot change since particles cannot pass through one another. Consequently, we confine our discussion of “ergodicity” to examining the time for which each particle has a given momentum, and ignore the position variables.

The density of occupied momentum states is defined as

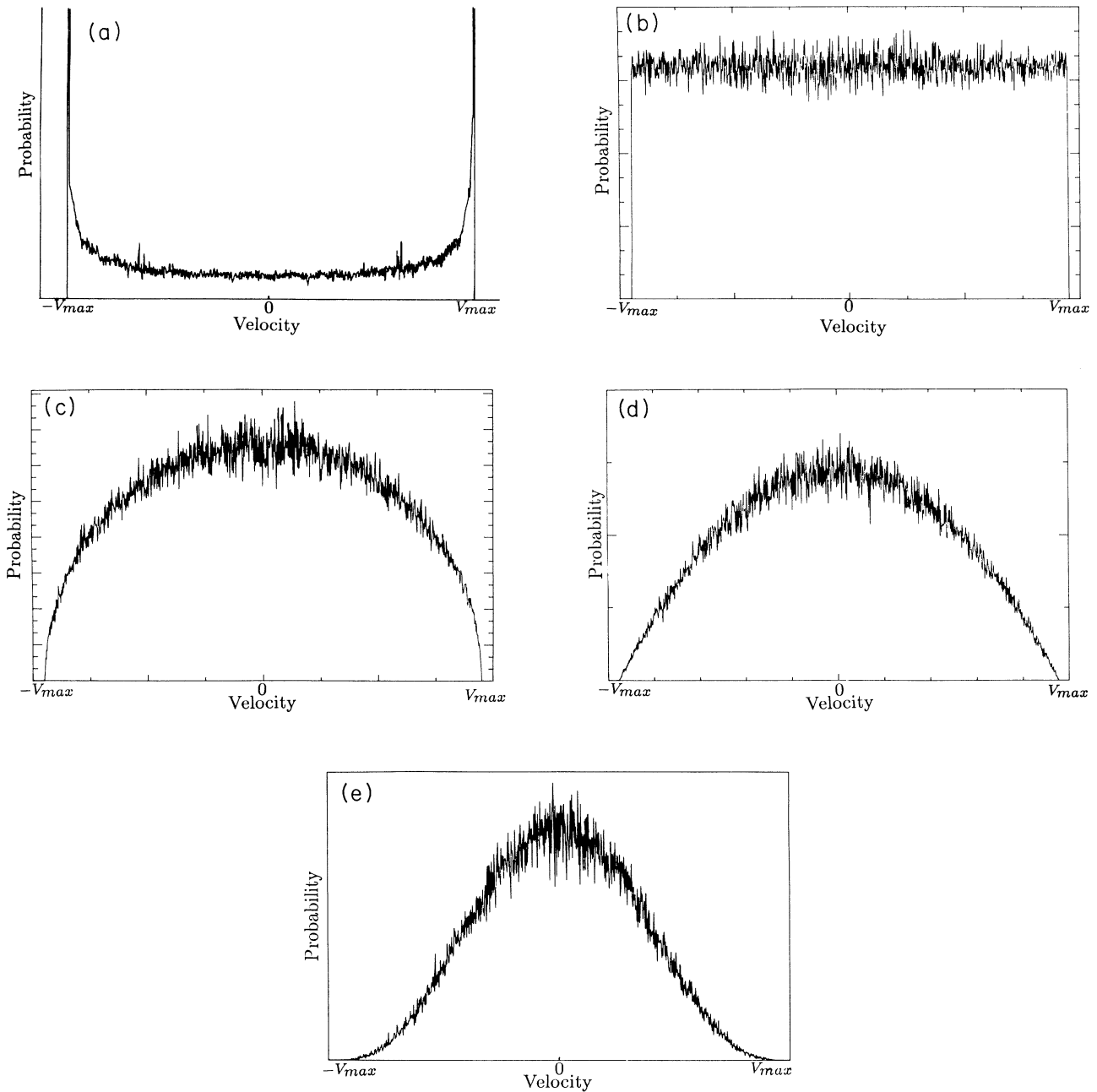


FIG. 1. Typical occupation probability of various momentum states for a single particle m_1 out of a total N . (a) $N=3$, $m_i=2,5,3$; (b) $N=4$, $m_i=2,3,4,6$; (c) $N=5$, $m_i=2,4,3,6,5$; (d) $N=6$, $m_i=2,3,4,5,3,6$; (e) $N=10$, $m_i=2,6,4,5,3,6,4,2,7,3$.

the time for which a given particle moves with each momentum. This is plotted in Fig. 1 for one particle out of three, four, five, six, and ten. These figures represent a projection of the density of occupation in momentum space onto one axis. The athermal nature of the system means that the units of time and momentum are arbitrary. The length of the ring is normalized to 1, which is all free volume because we are dealing with point particles.

In addition the special case of mass ratio 3:2:1 is plotted in Fig. 2. The spiky form of the latter graph shows the nonergodic nature of this case. Closer examination of the data shows that exact recurrence of the initial state occurs aperiodically. In each case the density of states is found from simulations sampling over a million different microstates. These are typical of the hundreds of different simulations we have performed to examine the various properties. The noise on these graphs decreases with run lengths, and the results are independent of the initial velocities and positions.

From Fig. 1 it is clear that the form of the density of states is strongly dependent upon the number of particles in the system. Analysis of these graphs shows that the three-particle case has form

$$n(p) \propto (p_{\max}^2 - p^2)^{-1/2}. \quad (8)$$

In the quantum limit, for motion on a closed loop of circumference L , we would expect to find states of wave number $2\pi n/L$. In the classical limit, which we are examining here, we anticipate that allowed states will be evenly distributed in momentum space. There are, however, two constraints placed on the system by momentum and energy conservation. For the three-particle case, these mean that the only states accessible to the system lie along an ellipse in p_1, p_2, p_3 momentum space which satisfies

$$p_1 + p_2 + p_3 = 0 \quad (9)$$

and

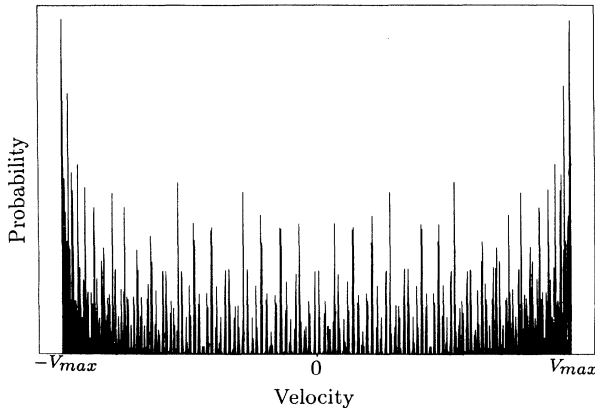


FIG. 2. Occupation probability of various momentum states for particle of mass 1 in the nonergodic, three-particle special case $m_1 = 1, 2, 3$.

$$p_1^2/2m_1 + p_2^2/2m_2 + p_3^2/2m_3 = E. \quad (10)$$

When this ellipse is projected onto, say, the p_1 axis it gives rise to a density of states $n(p_1)$ of the form given in Eq. (11) where p_{\max} is the largest possible value of p_1 consistent with the conservation laws.

The four-particle case [Fig. 1(b)] is simply a straight line, the five-particle case is elliptical [Fig. 1(c)], the six-particle case quadratic [Fig. 1(d)]. As the number of particles becomes larger the density of states tends towards the expected normal distribution [Fig. 1(e)]; as one expects for a one-dimensional infinite system [16]. This behavior can be explained by assuming a uniform density of states in momentum space with sampling limited by the conservation laws. The projection of an $(N-2)$ -dimensional ellipsoid onto a single axis in an N -dimensional space gives a density of states of general form:

$$n(p) \propto (p_{\max}^2 - p^2)^{(N-4)/2}. \quad (11)$$

These projections are, of course, equivalent to integrating (p_1, \dots, p_N) over all but one of the momenta. Thus the density of states can be explained by assuming a uniform distribution in *constrained* momentum space.

It is interesting to compare this analysis with that presented recently for the microcanonical ensemble momentum distribution [17]. The density of states is given by

$$n(p) \propto (p_{\max}^2 - p^2)^{(N-3)/2}, \quad (12)$$

which means that the density of states in the present case is isomorphic to that in the microcanonical ensemble *with one fewer particle*. This arises because there is an additional constraint of momentum conservation within the system considered here. This reduces by one the dimensionality of the accessible region of momentum space.

It is, of course, possible to obtain Eq. (3) by ensemble averaging using these densities of states. In the case of each particle having a different mass, consideration of Eq. (11) shows that $\langle E_i \rangle$ is the same for all particles except for a scaling factor of $p_{\max}^2/2m_i$. Solving for p_{\max}^2 from Eqs. (9) and (10) is difficult, requiring in general a solution of a multimimum problem, but as an illustration we consider here a system where symmetry allows an analytic solution.

Consider a system containing N particles of mass m_0 and one particle of mass m_1 . It is trivial to see that for a given energy in the system, the maximum momentum of m_1 occurs when all the other particles have the same velocity, call it v . In that case, $p_{1,\max}^2 = Nm_0v$ and $E = p_{1,\max}^2/2m_1 + Nm_0v^2/2$. Combining these expressions gives

$$\frac{p_{1,\max}^2}{2m_1} = \frac{Nm_0}{m_1 + Nm_0} E, \quad (13)$$

which is just the scaling factor required to make the time-averaged energy of m_1 consistent with Eq. (3).

IV. MATRIX REPRESENTATION

We have found that it is possible to map the system onto a group of matrices. These matrices provide a powerful method for analyzing the evolution of the system, and enable us to find and explain nonergodic special cases.

In the three-particle case, the outcome of each collision can be represented by the operation of a self-inverse 3×3 matrix on a vector of momenta (p_1, p_2, p_3) (note that this is not a momentum vector, but represents a state in phase space). Any sequence of collisions can be mapped onto a product of such matrices. In general, there are N such $N \times N$ matrices for a system of N particles since the ordering of the particles on a 1D ring cannot be altered. By applying the momentum conservation law it is possible to reduce by one the order of the matrices. The energy conservation law cannot be used in this way because it is nonlinear in p_i . The 3×3 and 2×2 representations for the three-particle system acting on (p_1, p_2, p_3) and (p_1, p_2) are as follows:

$$\begin{pmatrix} \alpha & 1+\alpha & 0 \\ 1-\alpha & -\alpha & 0 \\ 0 & 0 & 1 \end{pmatrix}, \quad \begin{pmatrix} \beta & 0 & 1+\beta \\ 0 & 1 & 0 \\ 1-\beta & 0 & -\beta \end{pmatrix}, \quad (14)$$

$$\begin{pmatrix} 1 & 0 & 0 \\ 0 & \delta & 1+\delta \\ 1 & 1-\delta & -\delta \end{pmatrix},$$

$$\begin{pmatrix} \alpha & 1+\alpha \\ 1-\alpha & -\alpha \end{pmatrix}, \quad \begin{pmatrix} -1 & -1-\beta \\ 0 & 1 \end{pmatrix}, \quad (15)$$

$$\begin{pmatrix} 1 & 0 \\ -1-\delta & -1 \end{pmatrix},$$

where

$$\alpha = \frac{m_1 - m_2}{m_1 + m_2}, \quad \beta = \frac{m_1 - m_3}{m_1 + m_3}, \quad \delta = \frac{m_2 - m_3}{m_2 + m_3}. \quad (16)$$

Thus in the three-body case there are three such matrices, representing collisions between particles 1-2, 2-3, and 3-1. If these matrices form part of a finite group we can deduce that the system is nonergodic.

Denoting these matrices by A , B , and C , respectively, we find the general relationship $ABCABC = I$ for all m_i . We can thus represent the possible states of the system as points on a 2D honeycomb lattice (Fig. 3). A particular starting condition results in an evolution represented by a walk along that lattice. At each node we reach a bifurcation (particle 1 can next strike either 2 or 3, depending on the initial conditions). Figure 3 suggests that the states of two systems taking opposite paths at a bifurcation will tend to drift apart rather than reconverge. These discrete bifurcations in trajectories destabilize calculation of the Lyapunov exponents. It should be noted that the evolution is not a random walk on the lattice, because after a collision of type A , particles 1 and 2 are moving apart and therefore the next collision cannot be of type A . Moreover, it is not genuinely even a directed random walk, since the next step is not independent of the previ-

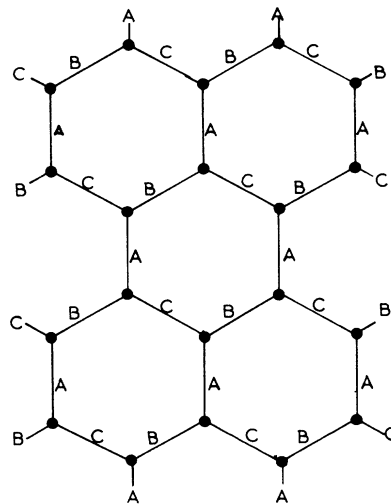


FIG. 3. Evolution of the three-particle system away from the initial state within the matrix group including A , B , and C represented by a walk on a hexagonal lattice.

ous steps. Henceforth, we shall describe this walk as a “chaotic walk,” since it is deterministic but the numerous bifurcations make it extremely sensitive to initial conditions.

In spite of all this, the walk along a hexagonal lattice escapes from its starting point sufficiently quickly to ensure that the system will move away from its initial state with a vanishingly small probability of ever returning (but see below for special cases wherein the honeycomb folds back on itself).

V. RANGE OF MOTION

In Fig. 4 we show the probability of finding each particle in a given section of the ring by way of a histogram plot of arc segments against the time spent in each segment during a run of 10^6 collisions. The ring was divided up into 1000 segments, but the histogram runs from 0 to 2000 to allow peaks straddling the origin to be shown unbroken. This means that the segment x is exactly equivalent to segment $x + 1000$. From this data we can extract a mean position and rms deviation of each particle. Zero total angular momentum prevents the particles from winding around the ring and ensures that the concept of a mean position is meaningful. Again, for this athermal system the time units are arbitrary.

Notwithstanding the difference in masses, numerous simulations show that the centers of the ranges of motion of the particles are equally spaced around the ring. Figure 4 is a typical result. This is an interesting result, since it suggests a long-range periodic ordering has occurred which could be interpreted as crystallization. Of course, the particles have no attractive interaction, so this ordering is driven purely by maximizing the entropy, as occurs in colloidal crystals [18,19].

The particles can move a considerable distance from their mean positions. Our empirical result of averages

taken over a great many simulations in the three-particle case is that the region in which each particle moves is proportional to the mean energy of that particle. For higher numbers of particles no simple rule was found; with particle mass, heavier near-neighbor particles tended to reduce the range of motion.

In general, the heavier particles remain closer to their mean position than the lighter ones. This is what one might expect since they are on average slower moving and the mean positions of the atoms are equally spaced.

In the two-particle case there is no overlap of the particles' range of position. In the three-particle case the overlap gives rise to a linear decay of occupation probability from a peak which is not the mean position. The steepness of this slope is greater if the mass of the adjacent particle is greater. Each segment of the ring can be occupied by either of two particles—an alternate viewpoint is to say that each segment is forbidden to one of the particles.

For more than three particles the extent of the range of

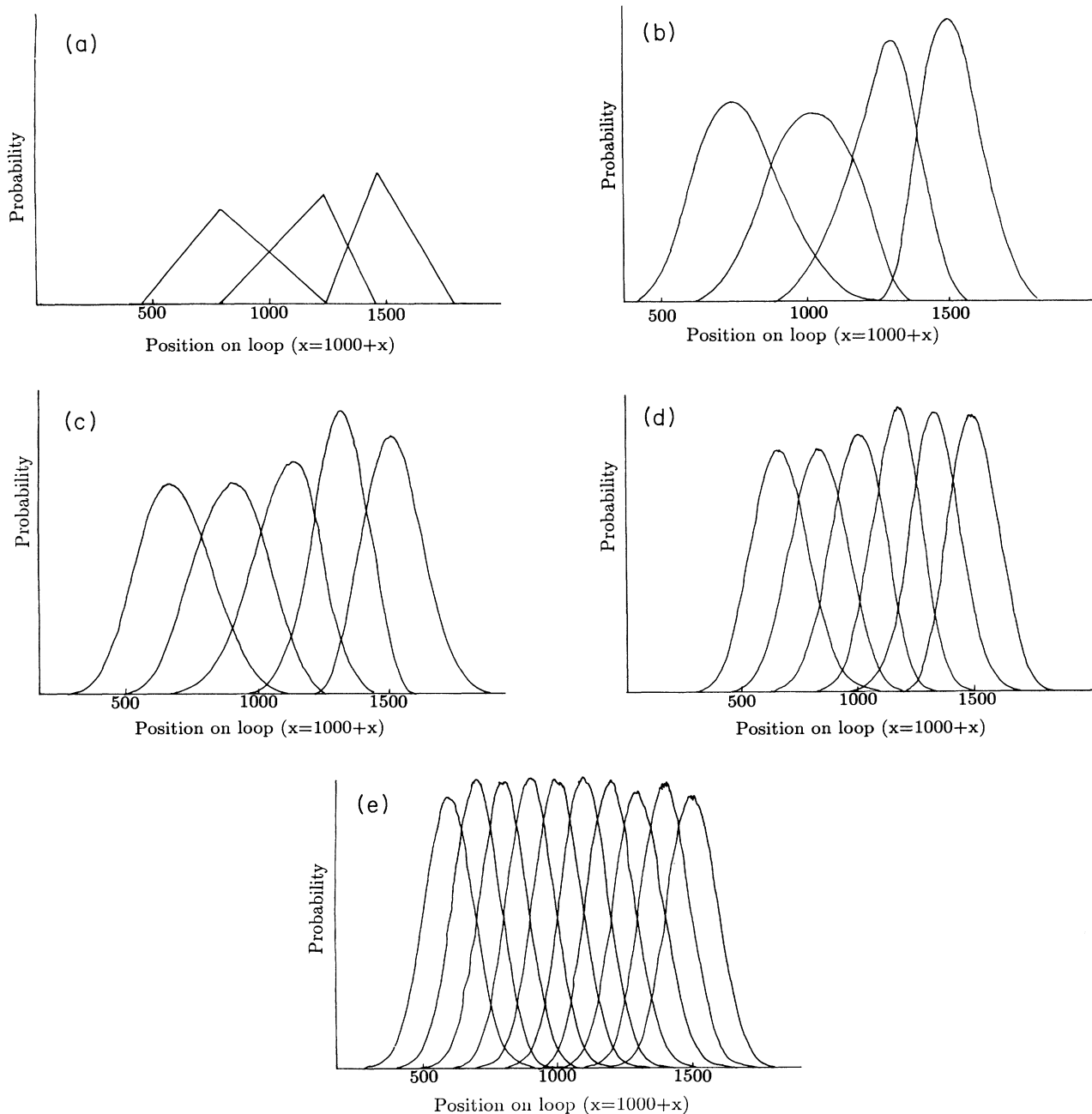


FIG. 4. Occupation probability of various segments of the loop by each particle (a) $N=3$, $m_i=1,2,3$; (b) $N=4$, $m_i=2,3,4,6$; (c) $N=5$, $m_i=2,4,3,6,5$; (d) $N=6$, $m_i=2,3,4,5,3,6$; (e) $N=10$, $m_i=2,6,4,5,3,6,4,2,7,3$.

motion is more complex. It appears that in addition to confinement of heavier particles, there is also a tendency for those particles whose neighbors are especially massive to be more strongly confined.

The equal spacing of the mean position of the particles around the ring will be altered if they are of finite size. This change is fairly simple: the length of the N th particle is simply added to the separation between the $(N-1)$ th and $(N+1)$ th particles. The free volume available to each particle remains unchanged.

VI. SPECIAL CASES

In general, an exact recurrence of the initial state does not occur after a long period of time. However, particularly in the three-particle problem, there are numerous special cases of the system which do lead to exact recurrence of the initial conditions. It is useful to view these within the matrix framework developed above, since they all require some extra relationship between the collision matrices.

A. Two particles

This is an almost trivial case, but it already reflects some of the properties which are found with more particles. There are two variables (p_1 and p_2) with two constraints. Thus the accessible region of momentum space is zero dimensional [it turns out to be two points $(x, -m_1x/m_2)$ and $(-x, m_1x/m_2)$]. Notwithstanding this lack of complexity and periodic behavior, the system still obeys Eq. (3) within the periodic boundary constraint.

In the matrix representation there is only one possible collision type (and hence only one matrix). This matrix is self-inverse, so it forms a two-element group with the identity. The two-particle system will always return to its initial state, but since there are only two states which satisfy the conservation laws, the system could be regarded as ergodic.

B. Identical masses

In the case of identical masses the system is nonergodic but Eq. (3) is again obeyed. Indeed, since all the m_i are the same, all the $\langle E_i \rangle$ are the same as expected in the standard equipartition theorem.

There are only a finite number of allowed states. This is because in any elastic collision between particles of equal mass the momenta are simply exchanged. In the matrix representation, the vector of momenta always contains the same elements in various permutations (in general all permutations are accessible). For three particles there are only six accessible states in momentum space (for N particles there are $N!$ states).

Unlike the two-particle case, there is no periodic solution, only a quasiperiodic one. If one considers the energies given initially to each particle, it is clear that these energies are transmitted around the loop without being scattered, and move with different velocities—they can be regarded as the limiting case of solitons. If the initial

momenta are at an irrational ratio to one another, there will be no periodicity in the recurrence of the initial state.

C. Three particles, mass ratio 3:2:1

There are an infinite number of special cases in the three-particle system which obey Eq. (3) but are not ergodic. They are therefore exceptions to Sinai's theorem [20]. Here we study one in detail. For ratio 3:2:1, the collision matrices are

$$\begin{pmatrix} \frac{1}{5} & \frac{6}{5} \\ \frac{4}{5} & -\frac{1}{5} \end{pmatrix} \begin{pmatrix} -1 & -\frac{3}{2} \\ 0 & 1 \end{pmatrix} \begin{pmatrix} 1 & 0 \\ -\frac{4}{3} & -1 \end{pmatrix}. \quad (17)$$

In addition to the matrix relation $ABCABC=I$, these give rise to the additional constraint $BCBC=-I$. The effect of this constraint is to collapse the hexagonal net representation of Fig. 3 onto a ladder (Fig. 5, strictly each point on this ladder represents two points in phase space with opposite velocities). Even so the matrices for this system are clearly part of an infinite group, and from a random walk analysis we might expect that the system will never return to its initial state.

This is not the case, however. The density of occupied states over 10^7 collisions shown in Fig. 2 has a distinctly nonergodic look, and detailed analysis of the microstates shows that an aperiodic exact recurrence of the initial state occurs. The reason is that the route by which the system leaves the initial state contains disproportionately few type- A collisions; type- A collisions are between the two heaviest (and therefore slowest moving) particles. In practice there are more type- B and $-C$ collisions, so the walk is biased. This is necessary but not sufficient to ensure exact recurrence. It requires that between type- A collisions there are more likely to be an even number of B and C collisions than an odd number, a condition which cannot be obtained by a Markovian collision probability. This being so, the result that the system cannot escape from its initial state which recurs (exactly) aperiodically

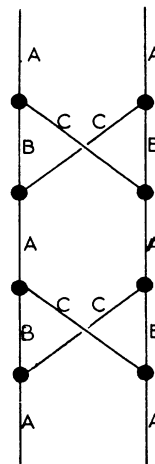


FIG. 5. Lattice on which evolution of the three-particle system $m_i=1,2,3$ away from the initial state within the matrix group including A , B , and C can be represented.

is evidence of a history-dependent collision probability.

There is no such direct evidence of history dependence in the general cases because the chaotic walk (and also a random walk) on the hexagonal lattice diverges much more quickly than does the walk on the ladder.

The sequence *BCBC* acts as a time reversal operator, keeping the particle speeds unchanged while reversing their sign. Since the positions are not restored exactly, the system is not totally time reversed, but there is a tendency for previous momentum states to be retraced.

In spite of the limited number of states which the system occupies, and the consequent nonergodicity, it still obeys the Eq. (3) condition derived above by differential occupation of the various accessible states. Maintaining this average provides the extra condition (after the conservation laws) which forces the system to recur.

From the collision matrices above it is easily shown that the constraint $BCBC = -I$ occurs in all systems where the masses obey the relation $m_1/m_3 = (m_2 + m_3)/(m_2 - m_3)$. Hence recurrence of the initial state will occur in an infinite number of systems obeying the relation above and the additional requirement that collisions of type *A* are between the heaviest two particles and are therefore the least frequent. Examples of this include mass ratios 10:3:2 and 12:5:3.

Other constraints give rise to special cases, for example, when all but one particle has the same mass. The matrix representation enables a rapid check to determine whether any system is a special case.

VII. DISCUSSION

It has been shown that for closed one-dimensional systems or those with periodic boundary conditions the law of equipartition has to be modified to Eq. (3). One of the effects of a closed system or one with periodic boundary conditions is to enforce conservation of momentum. If the system is ergodic, we can apply statistical mechanics to a constant energy-number-momentum-volume ensemble which leads to (3). This ensemble is sometimes referred to as a molecular-dynamics ensemble [14]. Equation (3) has been shown to have a broader validity, extending to nonergodic cases.

The density of states has been shown to be due to an

even distribution in a momentum-only phase space, where only part of that phase space is accessible because of constraints due to conservation of energy and momentum. These constraints are severe in cases with small numbers of particles, exceptionally so in the three-particle case, where they cause singularities in the projection of the density of states onto a single momentum at the maximal velocities [Fig. 2(a)].

Soliton-type solutions exist in the case where all masses are the same, but the solitons are rapidly destroyed in elastic collisions between particles of different masses. This dispersion of solitons is slower in the case where the masses are similar—an effect which has been observed in the larger scale system [11].

The system can be represented by a set of matrices representing each collision, and hence onto a “chaotic walk” on a lattice which depends on the number of particles present. This walk does not, in general, return. It is not truly random, however, since its sampling of the lattice produces the energy distribution given in Eq. (3). Since the system is deterministic, the walk is not random.

The recurrence of the initial state in a special case which maps onto a linear chain also suggests that this “chaotic walk” is not random.

Exact recurrence of the initial state does not occur (although of course the usual Poincaré recurrence exists) except in special cases where extra relationships exist between the collision matrices. Even when exact recurrence is obtained and only a limited number of states are accessed by the system, Eq. (3) still holds.

The effects studied here can be regarded as finite-size effects in the sense that they are most pronounced for small numbers of particles, and are probably avoided in large systems. The distortion to the equipartition law caused by periodic boundary conditions has more serious implications for molecular-dynamic simulations, since it causes an underexcitement of the more massive particles (in interacting systems these are equivalent to low frequency modes). In simulations of molecules, there will, in general, be a different temperature associated with rotational and translation degrees of freedom, and simulations of a single large particle surrounded by lighter particles will show significant deviations from equipartition.

-
- [1] L. Galgani and A. Scotti, *Riv. Nuovo Cimento* **2**, 189 (1972).
 - [2] M. Toda, *Nonlinear Waves and Solitons* (KTK, Tokyo, 1989).
 - [3] E. Fermi, J. Pasta, and S. Ulam, *Lect. Appl. Math.* **15**, 143 (1974).
 - [4] J. L. Lebowitz and J. K. Percus, *Phys. Rev.* **155**, 122 (1967).
 - [5] J. L. Lebowitz, J. K. Percus, and J. Sykes, *Phys. Rev.* **171**, 224 (1968).
 - [6] J. J. Erpenbeck and E. G. D. Cohen, *Phys. Rev. A* **38**, 3054 (1988).
 - [7] A. Monge, J. J. Erpenbeck, and E. G. D. Cohen, *Phys. Rev. A* **43**, 2031 (1988).
 - [8] A. Patrascioiu and A. Rouet, *Phys. Rev. A* **27**, 462 (1983).
 - [9] G. Benettin, G. L. Vechio, and A. Tenenbaum, *Phys. Rev. A* **22**, 1709 (1980).
 - [10] P. Bocchieri, A. Scotti, B. Bearzi, and A. Loinger, *Phys. Rev. A* **2**, 2013 (1970).
 - [11] J. Masoliver and J. Marro, *J. Stat. Phys.* **31**, 565 (1983).
 - [12] G. Benettin, L. Galgani, and A. Giorgilli, *Phys. Lett. A* **120**, 23 (1987).
 - [13] M. Aizenman, J. L. Lebowitz, and J. Marro, *J. Stat. Phys.* **18**, 179 (1978).
 - [14] T. Cagin and J. R. Ray, *Phys. Rev. A* **37**, 247 (1988).
 - [15] G. S. Pawley (unpublished).
 - [16] P. Resibois, *Mathematical Mechanics* (Gordon and Breach, New York, 1966).
 - [17] J. R. Ray and H. W. Graben, *Phys. Rev. A* **44**, 6905 (1991).
 - [18] H. N. W. Lekkerkerker, *Physica A* **176**, 1 (1991).
 - [19] P. N. Pusey, W. van Megan, S. M. Underwood, P. Bartlett, and R. H. Ottewill, *Physica A* **176**, 16 (1991).
 - [20] Y. G. Sinai, *Russian Math. Surveys* **25**, 137 (1970).